

A Novel Silicon Micro Amperometric Gas Sensor

Fariborz Maseeh, Michael J. Tierney, William S. Chu, Jose Joseph,
Hyun-Ok L. Kim*, Takaaki Otagawa

*Teknekron Sensor Development Corporation
Menlo Park, CA 94025, USA*

Abstract

We report on a silicon-based amperometric microelectrochemical gas sensor, based on an innovative design. This sensor shows a faster response (< 0.5 sec) to NO gas than other types of gas sensors, with good repeatability. A detection limit of 5 ppm is currently achieved for the first generation of these sensors.

Introduction

Amperometric sensors have been used to detect a wide range of electroactive gases, vapors, and liquids. The most well-known gas sensor of this type is the Clark oxygen sensor [1]. Amperometric gas sensors typically consist of three electrodes: working, counter, and reference. These electrodes are placed in contact with an electrolytic medium, such as an electrolyte solution, or a polymer electrolyte. A potential applied to the working electrode induces an electrochemical reaction of the sensed gas which generates a current, proportional to the gas concentration.

Selectivity for different gases may be achieved by employing: (1) different metals as the working electrode, (2) different applied electrode potentials, and (3) different polymer electrolytes. The working electrode selectivity is due to the differing ability of metals to electrocatalyze reactions of specific gases. For example, carbon monoxide can be oxidized on platinum, but not on gold, and some halocarbons are reduced only on silver. A second method of providing selectivity is by using different electrode potentials. In general, an electrochemical reaction will occur only beyond the characteristic half-cell potential of the reaction. Therefore, operating at the lowest possible potential will

reduce interference from other gases. In addition, the electrode may be biased anodically, or cathodically, to oxidize or reduce the gas respectively. The polymer electrolyte properties (e.g., pH, polarity) may also be used to detect gases. For example, proton-exchanged (H^+) Nafion is suitable for carbon monoxide [2], nitric oxide, and oxygen detection, while a neutral-pH electrolyte should be used for CO_2 or NH_3 detection. By a specific combination of the working electrode composition, sensor operating potential, and electrolytic medium, a fair amount of selectivity can be achieved with a very simple sensor.

Different sensor configurations have been designed to optimize relevant analytical parameters, such as response time, linear range, or operating lifetime. However, amperometric gas sensors have continued to suffer from rather slow response times (longer than several seconds). The slow response times are partly attributed to the gas-permeable membranes, which cover most of the sensors' areas, impeding gas diffusion to the electrodes. For example, conventional Clark-type oxygen sensors have typical response times of several seconds to a few minutes. The response times can be improved by integrating the gas-permeable membrane and internal electrolytes into one material using polymer electrolyte membranes; however, gas diffusion through such membranes is still slow.

Recently, several attempts have been made to develop planar-type micro-amperometric gas sensors by applying microfabrication techniques [2]; however, the early prototype of the sensors suffered from sluggish response and a short lifetime.

* Present address: Chemical Engineering Department, University of California at Berkeley.

An amperometric gas sensor has been designed [3] that eliminates gas diffusion through a membrane (or an electrolytic medium), and exhibits an enhanced lifetime. This innovative design, which is called the "back cell" configuration, results in very fast (< 0.5 sec) response times. In this paper we report on a version of this sensor, fabricated by using silicon micromachining. Response time and calibration curve data for nitric oxide detection are presented.

Experimental

Sensor design

To decrease the response time as much as possible, we have designed the back-cell sensor configuration. This design is shown schematically in Figure 1d. The unique feature of this design is that the sensed gas reaches the working electrode from the back side through a porous substrate rather than diffusing through a polymer electrolyte. As diffusion is at least five orders of magnitude faster in the gas phase than in an aqueous phase, response times are much faster with this design. In amperometric sensors, the gas must reach "triple points" of the sensor—sites where sensing electrode, polymer electrolyte, and gas phase meet—in order to react. In the sensor shown in Figure 1d, these triple points exist at the electrode end of each micromachined

pore. The uniformity and reproducibility of these triple points provided by the micromachining is much better than that obtained from other microporous substrate materials.

The design also allows the integration of a water reservoir with the sensor structure, resulting in a prolonged lifetime (over six months) when a Nafion film is used as the polymer electrolyte.

Sensor Fabrication

Fig. 1 illustrates a schematic of the micromachined gas sensor fabrication. Silicon wafers, 4 inch in diameter, (100) in orientation, and boron (p) doped ($7.5 - 12.5$ W.cm) are employed. The working gold electrode is sputtered on a 1 mm^2 bulk-micromachined (silicon / thermal oxide sandwich) membrane with prefabricated (etched) pores. The silicon membrane is a (100) orientation epitaxially grown silicon layer, $10\text{ }\mu\text{m}$ in thickness and of phosphorous (n) doping ($1\Omega\text{.cm}$) for electrochemical etch stop. Pores of 2 to $10\text{ }\mu\text{m}$ in diameters and up to $20\text{ }\mu\text{m}$ deep (in each case) were reactive ion etched with a chlorine-based chemistry with a chemical vapor deposited oxide etch mask. Fig. 2 shows a micrograph of an etched pore in silicon. The working, counter, and reference electrodes are made by sputtering a thin ($\sim 1000\text{ \AA}$) film of the appropriate metal.

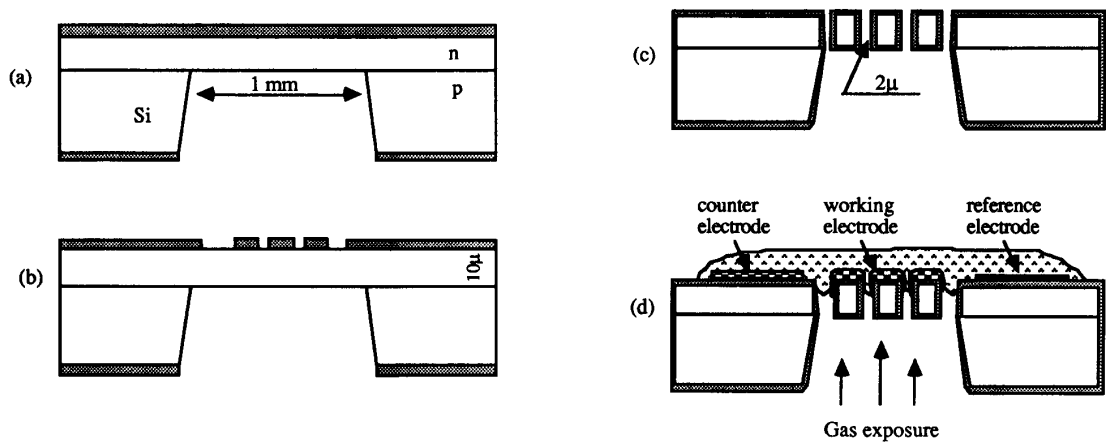


Fig. 1

Schematic of the gas sensor micromachining; views through wafer thickness; (a) anisotropic back-cell etch; (b) working electrode pore pattern; (c) etching of diffused layer, dielectric layer deposition; (d) metal and polymer electrolyte deposition, micromachined silicon electrochemical gas sensor.

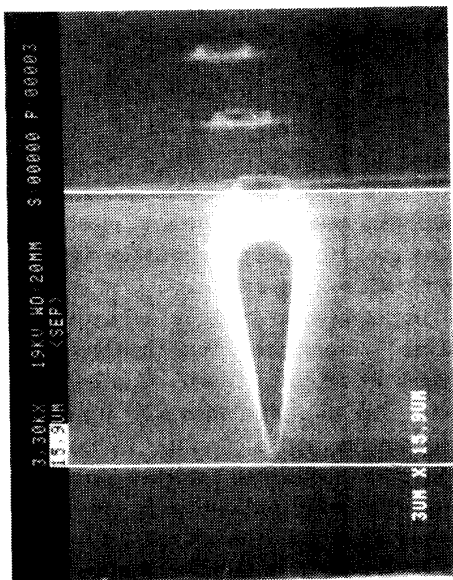


Fig. 2

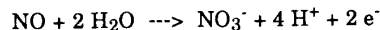
Reactive ion etched 3µm diameter pore in silicon using a chlorine-based chemistry and an oxide etch mask.

For the nitric oxide gas sensor, the working and counter electrodes are gold; the reference electrode is silver. The polymer electrolyte is H⁺-form Nafion. A gel of this polymer is made by slowly evaporating the alcohol solvent from a Nafion solution. The electrolyte is applied to the sensor substrate by mechanically spreading the gel onto the electrodes until it reaches a uniform thickness and consistency. Because the polymer electrolyte does not contain anions (aside from the bound sulfonate groups), the silver reference electrode is a silver silver-oxide electrode. Currently, the packaged sensor chip occupies a 1 cm² area. This area is expected to be reduced in subsequent versions of the sensor.

The NO sensor was tested in a custom-built gas handling system at a total gas flow rate of 1 l/min. The gas standard was 99.5 ppm NO in N₂. This gas could be diluted with N₂ further in the gas system to vary the NO concentration. The relative humidity of the gas flow past the sensor was 70 - 90%. To detect nitric-oxide gas, the working electrode was biased at +0.95 V versus the reference electrode with a Bioanalytical Systems CV-37 potentiostat. The current was monitored with a Macintosh computer and MacADIOS 411 A/D converter and interface.

Results and Discussion

To illustrate the advantages of the micromachined back-cell sensor, its use as a nitric oxide sensor is demonstrated. The potential placed on the working electrode was +0.95 V vs. the Ag/Ag₂O reference. At this potential, NO is oxidized:



A calibration curve from 0 to 100 ppm NO in N₂ is shown in Figure 3. This curve shows some sublinearity, although the correlation coefficient (R²) for the best-fit line is 0.983. Using this curve and the average noise observed from the sensor, the detection limit (based on S/N = 2) is estimated to be 5 ppm.

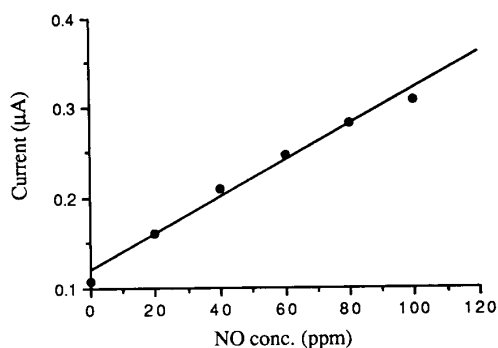


Fig. 3

Calibration curve for micromachined NO gas sensor

The response of this sensor is demonstrated in Figure 4. In this experiment, the response time of the sensor to 99.5 ppm of NO was measured at a total gas flow rate of 2 l/min. The sensor reaches 90% of its final value in 330 milliseconds (see Fig. 5), with a τ of 170 milliseconds (capacitance charging time-constant for 63.2% of impressed voltage). The recovery of the signal to baseline upon flushing of the NO from the sensor cell is also rapid. The recovery time is 550 milliseconds. The delay in the recovery is attributed to the out-diffusion of NO from the electrolyte polymer.

The results described above for the micromachined back-cell sensor compare favorably with other solid state sensors. Although the detection limit is larger than of semiconductor gas sensors, it is comparable to that typical of surface acoustic wave (SAW) devices. The

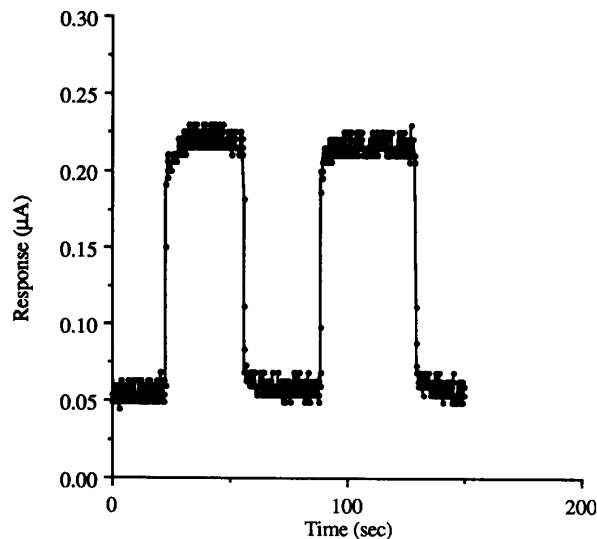


Fig.4

Microelectrochemical gas sensor response for NO at 99.5 ppm

response time is faster by several orders of magnitude than is observed for other types of gas sensors, which range from 1 to 1000 seconds.

Fig. 5 shows the normalized response of the micromachined silicon back-cell sensor compared with a porous ceramic-based back-cell sensor when exposed to 99.5 ppm NO. The silicon-based back-cell sensor shows a response time (90% of full scale) of 330 milliseconds compared with 6 seconds for a porous ceramic back-cell design.

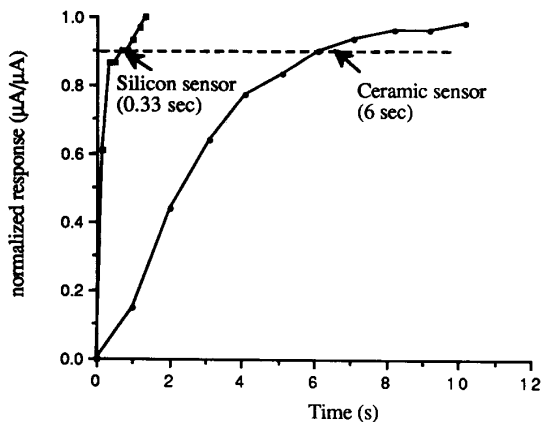


Fig. 5

Response time comparison of the silicon and a ceramic back-cell-based gas sensor for 99.5 ppm NO.

Because the working electrode is smaller (by a factor of four) in the silicon micromachined sensor, it consumes much less power than ceramic sensor (by a factor of fifteen).

Conclusion

The silicon micromachined sensor substrate offers advantages over other porous substrate materials, and even clearer advantages over macro-sized amperometric sensors. Because the substrate is made porous only on the working electrode, the bulk of the substrate can be rather thick to support the very thin silicon porous membrane. The thin membrane allows a shorter and therefore quicker diffusion path to the electrode compared to, for example, thicker porous ceramic substrates which have tortuous path pores. Response and recovery times are therefore reduced over back-cell sensors based on porous ceramic substrates [4]. The results reported here are obtained using an early prototype device whose geometric parameters are not optimized. Further optimization of the pore size and pore density is expected to result in improved sensitivity. Although this sensor is fabricated by micromachining, the present design does not benefit fully from the advantages of using microfabrication techniques. For example, the electrodes are rather large. By reducing the electrode area, and especially the inter-electrode gap width, the response time, sensitivity, and detection limit of this sensor could be improved further. A smaller inter-electrode distance would decrease the noise level of the sensor and, therefore, decrease the detection limit.

References

- [1] Clark Jr., L. C. "Monitor and control of blood and tissue oxygen tensions", *Trans. Am. Soc. Artif. Intern. Organs*, vol 2, (1956) pp. 41-57.
- [2] Otagawa, T. and Madou, M., Wing, S., Rich-Alexander, J., Kusanagi, S., Fujioka T., Yasuda, A., "Planar microelectrochemical carbon monoxide sensors", *Sensors and Actuators*, vol. B1, (1990), pp. 319-325.
- [3] Madou, M. J. and Otagawa, T. "Fast Response Time Microsensors for Gaseous and Vaporious Species" U. S. Patent # 4,812,221.
- [4] Kim, H.-O. L. and Tierney, M. J.: unpublished results.
- [5] Buttner, W. J., Maclay, G. J., and Stetter, J. R., "An integrated amperometric microsensor", *Sensors and Actuators*, vol. B1, (1990), pp. 319-325.